Growth of $Zn_x,Cd_{(1-x')}Se/Zn_xCd_yMg_{(1-x-y)}Se-InP$ quantum cascade structures for emission in the 3–5 μm range

W. O. Charles[a)]
The City College of New York, CUNY, New York, New York 10031

Y. Yao and K. J. Franz
Princeton University, Princeton, New Jersey 08544

Q. Zhang and A. Shen
The City College of New York, CUNY, New York, New York 10031

C. Gmachl
Princeton University, Princeton, New Jersey 08544

M. C. Tamargo
The City College of New York, CUNY, New York, New York 10031

(Received 1 October 2009; accepted 30 November 2009; published 23 March 2010)

The molecular beam epitaxial growth and electroluminescence (EL) properties of $Zn_{0.48}Cd_{0.52}Se/Zn_{0.24}Cd_{0.18}Mg_{0.58}Se$ quantum cascade (QC) structures are reported. The samples were composed of 30 repeats of a three-well active region. Cladding layers were inserted to isolate the core of the EL structure from the heavily doped contact region and to obtain optical confinement. Electroluminescence was observed in the 4–5 μm range. The observed narrowing of the electroluminescence linewidth was tentatively attributed, in part, to the incorporation of the ZnCdMgSe waveguide layers. A test sample consisting of multiple asymmetric coupled quantum well active regions separated by quaternary barrier layers was also investigated. The Fourier transform infrared (FTIR) absorption spectroscopy measurements suggest that QC structures with EL emission in the 3–4 μm range can be achieved with these materials. © *2010 American Vacuum Society.* [DOI: 10.1116/1.3276438]

I. INTRODUCTION

The production of high performance quantum cascade (QC) lasers in the 3–4.5 μm range is still a challenge due to the limited conduction band offset (CBO) of the lattice matched InGaAs/InAlAs material that is commonly used to fabricate these devices.[1,2] In order to overcome this problem, strain compensation has been explored as a means of increasing the CBO.[1–3] However, devices produced with strain compensation show a nonoptimum performance below 4.0 μm due to the presence of intervalley electron scattering. This has resulted in the exploration of other material systems with larger CBOs.[4–6] In this article, an alternative approach is presented in which the wide bandgap $Zn_{x'}Cd_{(1-x')}Se/Zn_xCd_yMg_{(1-x-y)}Se-InP$ material, a II–VI material system, is used. This II–VI material system is very promising because type-I multiquantum well structures can be readily grown lattice matched to InP with CBOs of as large as 1.12 eV.[7] Apart from having a large CBO, intervalley electron scattering does not interfere with the device operation. Therefore, this material system holds promise for producing highly performing devices with emission in the 3–5 μm range.

In the previous work, we have reported the observation of electroluminescence (EL) in this II–VI material system at 4.8 μm from 78 K up to room temperature.[8,9] The structures previously grown consisted of ten repeats of the active/injector period. No cladding layers were used. In that case, the full width at half maximum (FWHM) of the emitted light was quite broad (~52 meV) and, hence, gave cause for concern. Generally, a broad EL emission could be due to poor well/barrier interfaces or the result of cavity losses.[10,11] However, based on the presence of sharp photoluminescence (PL) spectra, with no discernible deep levels, and x-ray diffraction data that exhibit multiple satellite peaks for that EL sample, it is not suspected that the broadening is due to poor interface quality. Other possible factors include nonoptimal device design. In an effort to obtain better EL emission properties, several new samples were grown, this time with 30 repeats of the active/injector region. Also, cladding layers were added to minimize light interaction with the heavily doped contact layers and enable light confinement within the core of the QC structure. Here, we report the EL properties of these improved-design structures. We also report the Fourier transform infrared (FTIR) absorption properties of a special test sample designed for transitions in the 3.0–4.0 μm wavelength range.

II. EXPERIMENT

The CBO for $Zn_{0.48}Cd_{0.52}Se/Zn_{0.24}Cd_{0.18}Mg_{0.58}Se$ used in this work is 0.82 eV, while the effective masses for the well barrier material are 0.1892 and 0.1292, respectively.[12] Using these material parameters, a test sample was grown to assess

a)Electronic mail: wocharles99@aol.com

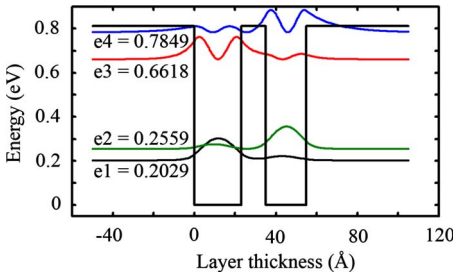

FIG. 1. (Color online) Simulation results showing the modulus square of the wave function for the A2732 test sample. The simulation results for the unbiased test sample at 300 K (**110**/2̲3/**12**/2̲0) predict **e1-e3** and **e2-e3** intersubband transitions at 0.449 and 0.406 eV, respectively.

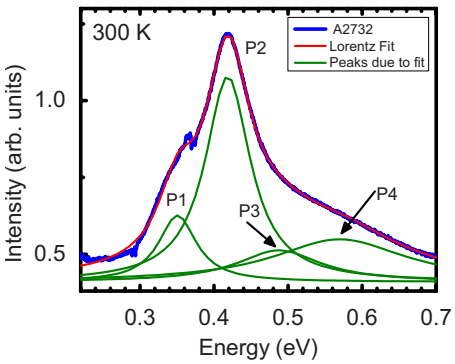

FIG. 3. (Color online) FTIR absorption spectrum for the A2732 test sample at 300 K. Lorentzian fit was performed to identify the absorption peak. The absorption energy corresponding to the identified peaks can be seen in Table I.

the accuracy of the simulation results at short wavelengths and demonstrate the possibility of transitions in the 3.0 μm range. The test sample had thick quaternary barrier layers separating two-well active regions, rather than the more complex injector structure grown for the EL structures. The layer sequence for one period of the test sample designed for absorption at 3.06 μm is as follows: **110**/2̲3/**12**/2̲0, where the layer thickness is given in angstroms, the barrier layers are indicated in bold, and the doped wells are underlined. A simulation based on the Schrödinger equation and the transfer matrix technique was used to predict the energy level distribution in this test sample. The results of this simulation can be seen in Fig. 1. The asymmetric coupled quantum wells of the test sample were repeated 30 times and the wells were doped ($n_{Cl} \sim 5 \times 10^{18}$ cm^{-3}) to enable FTIR absorption measurements.

The two-well active regions design of our earlier QC structures made it difficult to grow samples with **e1-e2** separation that is exactly resonant with the LO phonon energy ($\sim$32 meV) of the II-VI material. Therefore, in this study, the QC structure design was modified to contain three-well active regions to ensure better control of the lower lasing energy state separations. EL structures were designed for emission nominally at 3.35 and 4.87 μm to demonstrate coverage of the 3–5 μm atmospheric window. Calibration samples were grown to establish the desired alloy compositions, doping levels, and the CBO of the heterostructures. Further details on growth and calibration can be found in previous publications.[8,9]

These material parameters were also used to design three-well EL structures for emission at 3.35 and 4.87 μm. The layer sequences for one period of the 3.35 and 4.87 μm EL structures starting from the injection barrier are as follows: ***22***/*26*/***11***/*23*/***12***/*20*/***13***/17/**12**/15/**13**/14/**14**/13/**15**/11/**16**/10/**16**/9/**17**/8/**17**/8 and ***20***/*35*/***7***/*30*/***8***/*25*/**10**/20/**7**/18/**11**/16/**15**/15/**18**/15, respectively. The layer thicknesses are given in angstroms and the barrier layers are in bold. The Cl-doped layers are underlined and the active regions are in italics. Two cladding designs were explored. In the first, a 1.5 μm InGaAs:Si ($n \sim 1 \times 10^{17}$ cm^{-3}) layer was grown on the substrate side of the core, while a 0.23 μm $Zn_{0.48}Cd_{0.52}Se$:Cl ($n \sim 3 \times 10^{17}$ cm^{-3}) layer was grown on the side facing the top contact. The ternary layer was given a linearly graded doping profile. In the second design, 1.0 and 0.5 μm doped $Zn_{0.24}Cd_{0.18}Mg_{0.58}Se$:Cl ($n \sim 3 \times 10^{17}$ cm^{-3}) layers were grown at the substrate and top contact side of the EL structure, respectively. Shorter injector structures were also incorporated in the second sample to reduce the device resistance and doping requirements of the structure. Also, since the device gain is inversely proportional to the period length, a reduction in the injector length improves our chances of observing gain in this QC structure. The samples were grown in Riber 2300P dual chamber system in which one chamber is

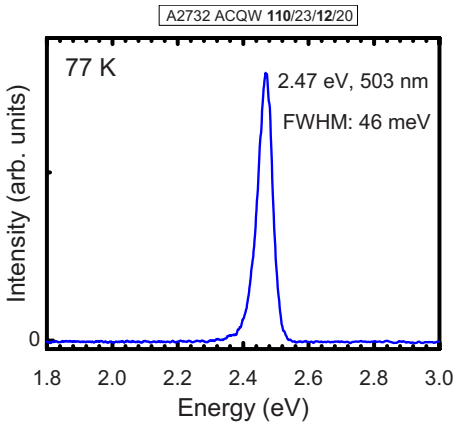

FIG. 2. (Color online) PL spectrum for the A2732 test sample. The absence of deep level emission indicates a low defect density.

TABLE I. Comparison between absorption peaks predicted by simulation and measured by FTIR for an unbiased test sample (A2732) at 300 K.

Energy transitions	Predicted (eV)	Measured (eV)
P1 (e2-e3)	0.4062 (3.06 μm)	0.3507 (3.54 μm)
P2 (e1-e3)	0.4589	0.4182
P3 (e2-e4)	0.5293	0.4877
P4 (e1-e4)	0.5820	0.5697

TABLE II. Summary of simulation results and the measured FTIR data for the A2710 and A2738 samples at zero bias (300 K). The EL results were obtained for the biased sample at 80 K.

Sample	Energy transitions	Predicted (eV) Unbiased	Measured (FTIR) (eV) Unbiased	Measured (EL) (eV) Biased
A2710	P1 (e3-e4)	0.3535 (3.51 μm)	0.329 (3.78 μm)	0.293 (4.23 μm)
	P2 (e1-e4)	0.4298	0.04149	⋯
	P3 (e1-e5)	0.5192	0.5068	⋯
A2738	e3-e4	0.225 (5.52 μm)	⋯	0.230 (5.40 μm)

used for III-V growth and another is used for II-VI growth. All grown samples were characterized using x-ray diffraction, PL, and FTIR spectroscopy.

III. RESULTS/DISCUSSION

The test sample (A2732) was subjected to PL analysis to assess the material quality. Excitation was performed with the 325 nm line of a HeCd laser. The absence of deep level emission in the PL spectrum, shown in Fig. 2, indicates that the material quality is good. This sample was processed into a multiple pass waveguide structure with 45° facets for FTIR absorption spectroscopy measurements, which were performed at room temperature. A Lorentzian fit was performed to identify the absorption peaks. The results, displayed in Fig. 3 and Table I, show a slight deviation between the predicted and the measured values. This may be due to monolayer scale fluctuations in the barrier width and/or to the fact that the simulation parameters for this material system are not fully opitmized.[12,13] The measured e2-e3 transition energy of 0.3507 eV suggests that a QC structure could be made to emit at ~3.5 μm using this material composition with only minor adjustments to the growth parameters.

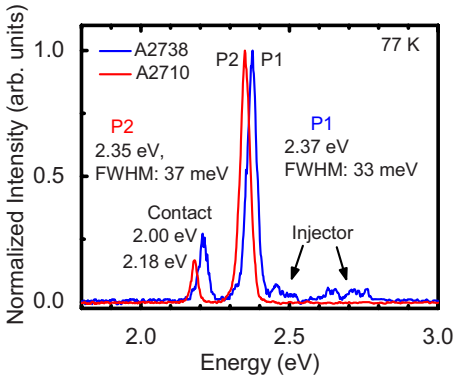

FIG. 4. (Color online) Photoluminescence spectrum for the A2710 and A2738 QC structures at 77 K. The dominant emission peaks from the active region were clearly visible when the samples were etched with a bromine/methanol solution. Lower intensity emission can be seen for the contact layer at 2.18 and 2.20 eV, respectively. Emission could also be detected for the injector layers of the A2738 sample.

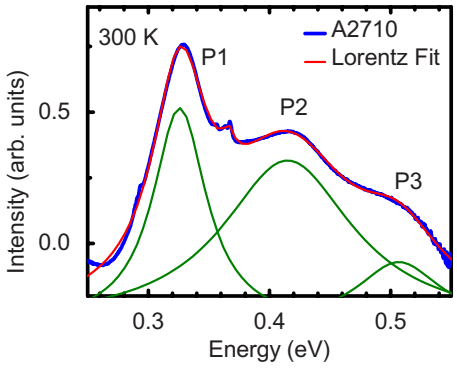

FIG. 5. (Color online) FTIR absorption spectrum for the A2710 unbiased sample at 300 K. Lorentzian fit was performed to identify the absorption peak. The absorption energy corresponding to the identified peaks can be seen in the Table.

The two EL samples (A2710 and A2738) were also investigated using PL and FTIR. In order to observe the PL emission from the core region of the EL structure, the thick contact layer was etched off using a dilute solution of bromine/methanol. The PL spectra for the A2710 and A2738 samples, using the 325 nm line of a He–Cd laser, are shown in Fig. 4. Again, the absence of a deep level emission indicates that the material is of high quality. Also, the FWHM of 36 and 33 meV that were obtained for these samples suggest that the well/barrier interfaces for these II-VI structures are of good quality. The FTIR absorption spectrum for the A2710 sample is shown in Fig. 5. Absorption peaks corresponding to **e1-e4** and **e3-e4** transitions were observed at 0.415 eV (2.99 μm) and 0.329 eV (3.78 μm), respectively, suggesting that QC emission at about 3.8 μm is possible.

The EL samples were processed into QC emitter structures. First, the samples were cleaned with oxygen plasma before Ti/Au contacts were deposited on the II-VI epilayer using e-beam evaporation. Ge/Au contacts were deposited on the substrate side. Following contact deposition, several photolithography steps were used to produce the final II-VI QC devices. Details of the device fabrication can be seen in Ref. 8. The *I-V* measurements made on the emitter structures

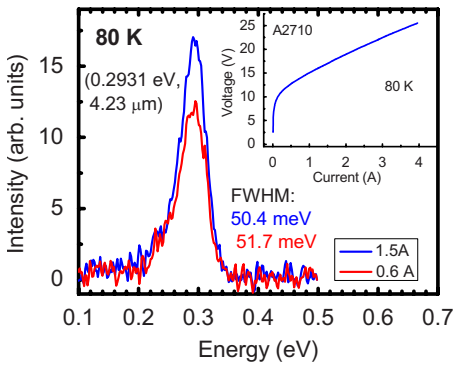

FIG. 6. (Color online) Electroluminescence emission for the A2710 sample at 80 K. Emission with a FWHM of 51 meV was observed at 0.2936 eV (4.23 μm) when a bias of 144 kV/cm was applied. The *I-V* curve for the device can be seen in the inset. The turn on voltages for the device is ~9 V at 80 K.

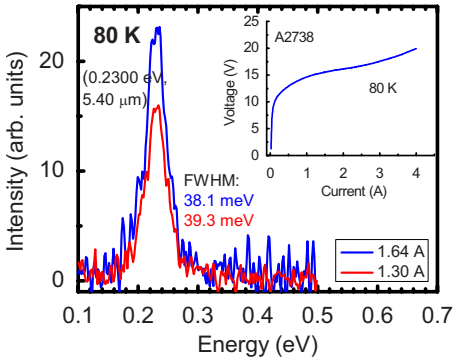

FIG. 7. (Color online) Electroluminescence emission for the A2738 sample at 80 K. Emission corresponding with a FWHM of 33 meV was observed at 0.2300 eV (5.40 μm) when a bias of 130 kV/cm was applied. The *I-V* curve for the device can be seen in the inset. The turn on voltages for the device is ~11 V at 80 K.

are shown as insets in Figs. 6 and 7. These measurements, made at 80 K, indicate the normal QC behavior. Using the FTIR in the step scan mode, the QC samples were investigated for emission at 80 K. Electroluminescence was observed for the A2710 and A2738 samples at 4.23 and 5.4 μm, respectively (see Figs. 6 and 7 and Table II). The EL emission for the A2710 sample has a FWHM of 51 meV, while the A2738 sample has a FWHM of 38.8 meV. Since the EL linewidth is related to the emission energy, a more accurate indication of quality is obtained from the ratio of $\Delta E/E$, where ΔE is the linewidth of the peak and E is the peak energy. The ratio $\Delta E/E$ was calculated for the EL spectra in Figs. 6 and 7, and values of 0.174 and 0.168 were obtained for the A2710 and A2738 samples, respectively. These numbers constitute a slight improvement over the $\Delta E/E$ of 0.201 calculated for our previously reported EL structure, which did not contain any cladding or waveguide layers.[8] We tentatively attribute this slight improvement in $\Delta E/E$ to the presence of an InGaAs waveguide layer in A2710 and ZnCdMgSe quaternary cladding layers in the A2738 sample (see Fig. 8). We believe that improvements in the waveguide and device structure design, as well as optimization of the doping levels in the core, will produce further improvements in the device properties.

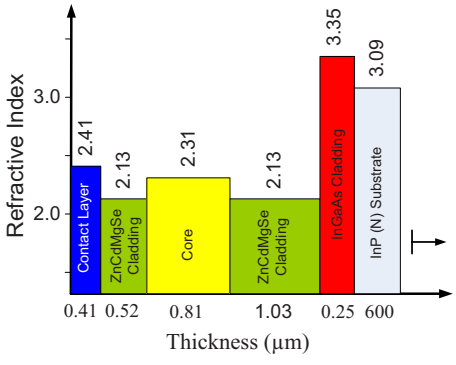

FIG. 8. (Color online) Index profile for the A2738 EL sample. The refractive index for the ternary and quaternary II-VI layers in the mid-IR were calculated using Ref. 14. The refractive index of the core was determined based on the percentage of ternary and quaternary material that in that region.

IV. SUMMARY/CONCLUSION

A test sample consisting of QC active regions separated by thick quaternary barrier layers was grown to investigate the possibility of producing QC structures that emit at the short wavelength end of the first atmospheric window (3–5 μm). The simulation results for the test sample predicted that the **e2-e3** electronic transition would be at 0.4062 eV (3.06 μm), while FTIR absorption for that sample was observed at 0.3507 eV (3.54 μm). The small discrepancy between the simulation and the FTIR data suggests that the II-VI material simulation parameters may need to be optimized. Nevertheless, these results confirm that QC structures with emission wavelengths between 3.0 and 4.0 μm can be produced using this II-VI material system. Two QC EL device structures designed for emission within the first atmospheric window were also grown and investigated for their electroluminescence properties. Emission was observed at 4.23 and 5.40 μm. Quaternary cladding layers were added between the core and the contact layers for the purpose of light confinement in the A2738 sample, while an InGaAs waveguide layer was used in the A2710 sample. A slight reduction in the value of $\Delta E/E$ was obtained for these new structures compared to our previously reported EL results. We conclude that improvement in the waveguide and device structure design, as well as optimization of the doping levels in the core, will result in improved EL characteristics.

ACKNOWLEDGMENTS

This work was supported by NSF Grant No. EEC-0540832 (MIRTHE-ERC) and by NSF Grant No. HRD-0833180 (CREST).

[1]J. Faist, F. Capasso, D. L. Sivco, A. L. Hutchinson, S. G. Chu, and A. Y. Cho, Appl. Phys. Lett. **72**, 680 (1998).
[2]J. S. Yu, A. Evans, S. Slivken, S. R. Darvish, and M. Razeghi, Appl. Phys. Lett. **88**, 251118 (2006).
[3]M. P. Semtsiv, M. Wienold, S. Dressler, and W. T. Masselink, Appl. Phys. Lett. **90**, 051111 (2007).
[4]J. Devenson, O. Cathabard, R. Teissier, and A. N. Baranov, Appl. Phys. Lett. **91**, 251102 (2007).
[5]J. Devenson, D. Barate, O. Cathabard, R. Teissier, and A. N. Baranov, Appl. Phys. Lett. **89**, 191115 (2006).
[6]D. G. Revin and J. W. Cockburn, Appl. Phys. Lett. **90**, 021108 (2007).
[7]M. Sohel, X. Zhou, H. Lu, M. N. Perez-Paz, M. C. Tamargo, and M. Munoz, J. Vac. Sci. Technol. B **23**, 1209 (2005).
[8]K. J. Franz, W. O. Charles, A. Shen, A. J. Hoffman, M. C. Tamargo, and C. Cmachl, Appl. Phys. Lett. **92**, 121105 (2008).
[9]W. O. Charles, K. J. Franz, A. Shen, Q. Zhang, M. C. Tamargo, and C. Gmachl, J. Cryst. Growth **310**, 5380 (2008).
[10]S. Tsujino *et al.*, Appl. Phys. Lett. **86**, 062113 (2005).
[11]J. Faist, F. Capasso, C. Sirtori, D. L. Sivco, A. L. Hutchinson, S. G. Chu, and A. Y. Cho, Appl. Phys. Lett. **65**, 94 (1994).
[12]M. Munoz, H. Lu, X. Zhou, M. C. Tamargo, and F. H. Pollak, Appl. Phys. Lett. **83**, 1995 (2003).
[13]J. D. Wu, J. W. Lin, Y. S. Huang, W. O. Charles, A. Shen, Q. Zhang, and M. C. Tamargo, J. Phys. D: Appl. Phys. **42**, 165102 (2009).
[14]T. Morita, H. Shinbo, T. Nagano, I. Nomura, A. Kikuchi, and K. Kishino, J. Appl. Phys. **81**, 7575 (1997).